

Influence of correlation effects on the magneto-optical properties of the half-metallic ferromagnet NiMnSb

S. Chadov,¹ J. Minár,¹ H. Ebert,¹ A. Perlov,² L. Chioncel,^{3,*} M. I. Katsnelson,⁴ and A. I. Lichtenstein⁵

¹Department Chemie und Biochemie, Physikalische Chemie, Universität München, Butenandtstrasse 5-13, D-81377 München, Germany

²Accelrys, 334 Cambridge Science Park, Cambridge CB4 0WN, England

³Institute of Theoretical Physics, Technical University of Graz, A-8010 Graz, Austria

⁴University of Nijmegen, NL-6525 ED Nijmegen, The Netherlands

⁵Institute of Theoretical Physics, University of Hamburg, Hamburg, Germany

(Received 15 September 2006; revised manuscript received 12 October 2006; published 31 October 2006)

The magneto-optical spectra of NiMnSb were calculated in the framework of the local spin density approximation (LSDA) combined with dynamical mean-field theory (DMFT). Comparing with results based on the plain LSDA, the additional account of many-body correlations via DMFT results in a noticeably improved agreement of the theoretical Kerr rotation and ellipticity spectra with corresponding experimental data.

DOI: 10.1103/PhysRevB.74.140411

PACS number(s): 75.50.Cc, 78.20.Ls, 71.20.Be, 71.15.Rf

Since the discovery of the giant magneto-optical Kerr effect¹ (MOKE) in PtMnSb magneto-optical properties became an important issue for the Mn-based family of Heusler alloys.^{2–10} However, despite the similar structure, the group of isoelectronic alloys PtMnSb, NiMnSb, and PdMnSb show quite different maximum amplitudes in their MOKE spectra.^{1,2} A theoretical description of the observed difference of the MOKE spectra became possible within *ab initio* band-structure calculations.^{8,10–12} However, although the various calculated MOKE spectra give reasonable qualitative agreement with experiment, one can notice that there exist several systematic discrepancies generally ascribed to the use of the local spin density approximation (LSDA). In particular, for NiMnSb, one can see that the low-energy peak of the Kerr rotation spectra at 1.4 eV is shifted to a regime of 1.6–2 eV. Also there is a noticeable deviation of the amplitude for the peak at 4 eV as well as in the intermediate energy regime. Among other reasons, the discrepancies encountered in LSDA-based results could appear due to an insufficient treatment of electronic correlations. For example, as was shown for bcc Ni,^{13,14} the account of local dynamical correlations is extremely important for a proper description of its MOKE spectra. In the case of NiMnSb the main contribution to the optical transitions comes from the *d* shell of Mn, which supplies the unoccupied part of the density of states (DOS). At the same time *d* electrons of Mn should be treated as locally correlated.¹⁵ Based on this supposition one can expect an improvement of MO spectra in NiMnSb by taking appropriate account of local correlation effects for the Mn *d* shell in band-structure calculations. In the present work the latter is implemented within the so-called dynamical mean-field theory (DMFT) approach.¹⁶

In our calculations the central quantity is the optical conductivity tensor $\sigma_{\lambda\lambda'}$, as all optical and magneto-optical properties can be expressed through its Cartesian components ($\lambda = \{x, y, z\}$). In particular, for the complex Kerr angle, which combines Kerr rotation θ_K and ellipticity ε_K , the following expression can be used:¹⁷

$$\theta_K(\omega) + i\varepsilon_K(\omega) \approx \frac{-\sigma_{xy}(\omega)}{\sigma_{xx}(\omega) \sqrt{1 + \frac{4\pi i}{\omega} \sigma_{xx}(\omega)}}. \quad (1)$$

In order to calculate the optical conductivity we use the expression for the Hermitian component derived for the zero-temperature case¹⁸ by implementing the Green's function formalism in Kubo's linear response theory.¹⁹

$$\sigma_{\lambda\lambda'}^{(1)}(\omega) = -\frac{1}{\pi V} \int_{\varepsilon_F - \hbar\omega}^{\varepsilon_F} d\varepsilon \text{Tr} \{ \hat{J}^\lambda \text{Im} G(\varepsilon + \hbar\omega) \hat{J}^{\lambda'} \text{Im} G(\varepsilon) \}, \quad (2)$$

where V is the volume of the spatial averaging and \hat{J}^λ is the current-density operator. $\text{Im} G(\varepsilon)$ stands for the anti-Hermitian part of the retarded one-electron Green's function. The Hermitian part of the conductivity tensor $\sigma_{\lambda\lambda'}^{(2)}(\omega)$ can be obtained via the Kramers-Kronig relations.

Formulation (2) is used because it allows one to include straightforwardly all correlations in the one-particle Green's function via the Dyson equation:

$$[\varepsilon - \hat{H}_0 - \hat{\Sigma}(\varepsilon)] \hat{G}(\varepsilon) = \hat{I}, \quad (3)$$

where \hat{H}_0 is the LSDA-based one-particle Hamiltonian including the kinetic energy, electron-ion interaction, and Hartree potential, while the self-energy operator $\hat{\Sigma}$ describes all static and dynamic effects of electron-electron exchange and correlations. The most popular approximation nowadays for the self-energy is DMFT which introduces it as a local, energy-independent exchange-correlation potential $V_{xc}(r)$. As the introduction of such an additional potential does not change the properties of H_0 we will incorporate this potential in H_{LSDA} and subtract this term from the self-energy operator. This means that the self-energy Σ describes exchange and correlation effects not accounted for within the LSDA.

The most straightforward and accurate way to solve Eq. (3) is to use the Korringa-Kohn-Rostoker Green's function (KKR GF) method.²⁰ However, subsequent calculations of

optical properties within the KKR GF method become very time consuming due to the energy-dependent matrix elements of the current-density operator. A possible alternative is to use the so-called variational or fixed-basis-set methods. Within such an approach the Green's function is represented as a sum over energy-independent basis functions $|i\rangle$:

$$G(\epsilon) = \sum_{ij} |i\rangle\langle i| \frac{1}{\epsilon - H_{\text{LSDA}} - \hat{\Sigma}(\epsilon)} |j\rangle\langle j| = \sum_{ij} |i\rangle G_{ij}(\epsilon) \langle j|, \quad (4)$$

with the Green's function matrix defined as

$$G_{ij}(\epsilon) = [\langle i|j\rangle\epsilon - \langle i|\hat{H}_{\text{LSDA}}|j\rangle - \langle i|\hat{\Sigma}(\epsilon)|j\rangle]^{-1}. \quad (5)$$

The dynamical correlation correction to the one-particle hamiltonian H_{LSDA} is represented via the energy-dependent self-energy operator $\hat{\Sigma}(\mathbf{r}, \mathbf{r}', \epsilon)$ which in general is a nonlocal quantity. Here, the self-energy is calculated via the DMFT approach¹⁶ which accounts only for local (on-site) correlations that are described within the Anderson impurity model (AIM).²¹ By linking the Green's function of the effective impurity to the single-site Green's function derived from the \mathbf{k} -space summation, DMFT provides a self-consistent method to determine the self-energy accounting for on-site correlations. The actual approximation made in DMFT is the substitution of the nonlocal (\mathbf{k} -dependent) self-energy by the single on-site component. The latter corresponds to the limit of infinite coordination. Fortunately, in many cases for three-dimensional systems this is a rather good approximation.²²

Although the formalism to be presented below is primarily used in connection with a site-diagonal self-energy, it should be stressed that any more complex self-energy can be used as well. In particular, the formalism is able to deal with a site-non-diagonal self-energy occurring, for example, within the *GW* approach.²³

Dealing with crystals, one can make use of Bloch's theorem when choosing basic functions $|i_{\mathbf{k}}\rangle$. This leads to the \mathbf{k} -dependent Green's function matrix:

$$G_{ij}^{\mathbf{k}}(\epsilon) = [\langle i_{\mathbf{k}}|j_{\mathbf{k}}\rangle\epsilon - \langle i_{\mathbf{k}}|\hat{H}_{\text{LSDA}}|j_{\mathbf{k}}\rangle - \langle i_{\mathbf{k}}|\hat{\Sigma}(\epsilon)|j_{\mathbf{k}}\rangle]^{-1}. \quad (6)$$

The efficiency and accuracy of the approach is determined by the choice of $|i_{\mathbf{k}}\rangle$. One of the most computationally efficient variational methods is the linear muffin tin orbital (LMTO) method²⁴ which allows one to get a rather accurate description of the valence and conduction bands in the range of about 10 eV, which is enough for the calculation of the optical spectra ($\hbar\omega < 6-8$ eV). As the method introduces site- and angular-momentum-dependent basis functions

$$\chi_{lm\mathbf{R}}^{\mathbf{k}}(\mathbf{r}) = \Phi_{lm}^{\mathbf{h}}(\mathbf{r} - \mathbf{R}) + \sum_{lm'\mathbf{R}'} h_{lm\mathbf{R},lm'\mathbf{R}'}^{\mathbf{k}} \Phi_{lm'}^{\mathbf{t}}(\mathbf{r} - \mathbf{R}'), \quad (7)$$

it perfectly fits any single-site approximation of the self-energy. The superscripts "h" and "t" stand for the so-called "head" and "tail" parts of the basis functions.

As the $\langle i|j\rangle$ and $\langle i|\hat{H}|j\rangle$ matrix elements in Eq. (6) are energy independent it is enough to calculate them only once for each \mathbf{k} point.

In the framework of the DMFT the self-energy operator can be expressed in the form

$$\hat{\Sigma}(\mathbf{r}, \mathbf{r}', \epsilon) = \sum_{l,\mathbf{R}\mathbf{R}'} \delta_{\mathbf{R}\mathbf{R}'} \sum_{mm'} \Theta(|\mathbf{r} - \mathbf{R}|) Y_{lm}^*(\mathbf{r} - \mathbf{R}) \times \sum_{lmm'}^{\mathbf{R}\mathbf{R}'}(\mathbf{r}, \mathbf{r}', \epsilon) \Theta(|\mathbf{r}' - \mathbf{R}'|) Y_{lm'}(\mathbf{r}' - \mathbf{R}'), \quad (8)$$

where $\Theta(r) = 1$ if \mathbf{r} is inside the atomic sphere and zero otherwise. Due to the special choice of LMTO basis functions (7) only the head component will give a significant contribution to the matrix elements of the self-energy operator (8), leading to an extremely simple \mathbf{k} -independent expression:

$$\langle \chi_{lm\mathbf{R}}^{\mathbf{k}} | \hat{\Sigma} | \chi_{lm'\mathbf{R}'}^{\mathbf{k}} \rangle \approx \int d^3r d^3r' \Phi_{lm}^{\mathbf{h}*}(\mathbf{r} - \mathbf{R}) \times \sum_{lmm'}^{\mathbf{R}\mathbf{R}'}(\mathbf{r}, \mathbf{r}', \epsilon) \Phi_{lm'}^{\mathbf{h}}(\mathbf{r} - \mathbf{R}). \quad (9)$$

The accuracy test of this approach was done in Ref. 13 and the error was found to be within 5% which is substantially less than the approximations made for the estimation of the self-energy itself.

The self-energy is calculated by using as an AIM solver the so-called spin-polarized *T* matrix plus fluctuation exchange (SPTF) approximation.^{25,26} This is a perturbative approach which provides an analytical technique to sum the infinite set of Feynman diagrams for the several types of interactions in a uniform electron gas. Fortunately, these sets of diagrams very often appear to be sufficient to describe the effects caused by dynamical correlations in moderately correlated shells like 3*d* electrons in transition metals^{14,27} as well as in systems with strong correlations.²⁹ This makes it a very attractive alternative to the so-called quantum Monte Carlo technique,³⁰ which sums all possible sets of diagrams of perturbation theory and therefore is much more time consuming.

The DMFT scheme is implemented within the KKR GF method, which allows one to use the advantages of the scattering theory formulation in the Green's function construction. For example, it is possible to calculate the self-energy in a self-consistent manner (parallel with the charge density).²⁷

Introducing the anti-Hermitian part of the Green's function matrix (6) $\text{Im}G_{ij} = \frac{1}{2}(G_{ij} - G_{ji}^*)$ and taking into account translational symmetry, the Hermitian part of the optical conductivity (2) is expressed as

$$\sigma_{\lambda\lambda'}^{(1)} = \frac{1}{\pi\omega} \int d^3k \int_{\epsilon_F - \hbar\omega}^{\epsilon_F} d\epsilon \sum_{ij} \mathcal{J}_{ij}^{\lambda}(\mathbf{k}, \epsilon) \mathcal{J}_{ji}^{\lambda'}(\mathbf{k}, \epsilon + \hbar\omega) \quad (10)$$

with

$$\mathcal{J}_{ij}^{\lambda}(\mathbf{k}, \epsilon) = \sum_n \text{Im} G_{in}(\mathbf{k}, \epsilon) \langle n_{\mathbf{k}} | \hat{J}^{\lambda} | j_{\mathbf{k}} \rangle. \quad (11)$$

Actually the possibility of splitting the $\mathcal{J}_{ij}^{\lambda}(\mathbf{k}, \epsilon)$ matrix elements into energy-dependent and -independent parts makes the calculation of optical conductivity rather fast.

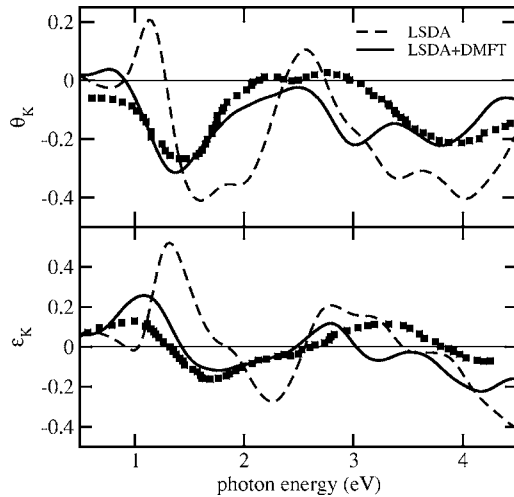


FIG. 1. MO spectra for NiMnSb. Upper panel: Kerr rotation angle. Lower panel: Kerr ellipticity. Broken line, LSDA calculations; solid line, LSDA+DMFT calculations. The square points represent the experimental results given in Refs. 1 and 2.

The calculation procedure is built up as follows. The energy-dependent on-site self-energy $\Sigma(\epsilon)$ is obtained from the self-consistent KKR GF scheme.²⁷ For a given self-energy the Dyson equation (6) is used to obtain the effective Green's function in the basis set of the LMTO method. The anti-Hermitian part $\text{Im}G_{ij}$ of the effective Green's function is used to calculate the matrix elements of the current-density operator in Eq. (11). The latter allows one to evaluate the optical conductivity given by Eq. (10). Spin-orbit coupling which is, together with exchange splitting, the actual source of MOKE, is taken into account via the second-variation technique.

The comparison between the MO spectra of NiMnSb calculated within the LSDA, LSDA+DMFT, and the experimental results is shown in Fig. 1. The obvious conclusion is that an account of local correlations is essentially important to describe correctly the positions as well as the magnitudes of both low- and high-energy Kerr rotation peaks (situated at 1.4 and 4 eV).

It is sufficient to consider in detail only the real part of the MOKE spectrum, i.e., the rotation, as the Kerr ellipticity is a related quantity. The Mn *d* shell indeed experiences noticeable dynamical correlations as depicted by the self-energy plot shown in Fig. 2 with the amplitudes of the imaginary component up to 4 eV. On the other hand, for a given crystal structure the correlation effects are maximal near half filling.²⁸ Since the Ni *d* states are almost fully occupied, inclusion of dynamical correlations does not influence the magneto-optical properties presented below. The effective Coulomb interaction is parametrized by $U=3$ eV and $J=0.9$ eV. Numerical tests show that approximately the same results are obtained within the range of $U=3\pm 0.5$ eV.

Considering Eqs. (10) and (11) we can straightforwardly analyze the modifications in the MO spectrum. As the matrix elements $\langle n_{\mathbf{k}} | \hat{J}^{\lambda} | j_{\mathbf{k}} \rangle$ are not influenced by DMFT, the two possible sources of the influence are the Green's function matrix and the change in the occupation numbers. However,

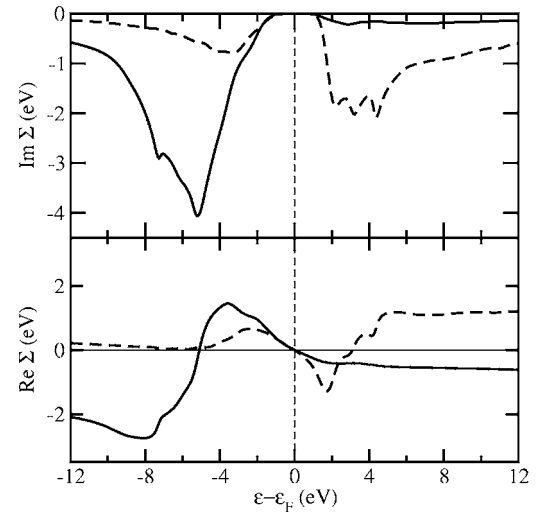


FIG. 2. Spin-resolved dynamical self-energy for Mn obtained from SPR KKR calculations using the SPTF solver. Lower panel, real component; upper panel, imaginary component. Solid and broken lines correspond to majority and minority spin components, respectively.

in the present calculations the number of occupied and unoccupied states for each spin projection is strictly conserved. This occurs due to the special construction of the self-energy represented by the so-called particle-particle channel.²⁶ The latter includes the channels of perturbation theory starting from the second order and that is it why it processes the dominant contribution in the dynamical correlations for the *d*-electron shell. This leads in particular to the conclusion that local correlations modify only the interband part of the optical conductivity. The intraband contribution (often called as Drude term) which is determined by the Green's function matrix elements at the Fermi level⁸ remains unchanged, due to the choice of the self-energy to be zero at the Fermi level (see Fig. 2) according to the double-counting treatment (Ref. 27). Thus, one can predominantly relate the changes in the

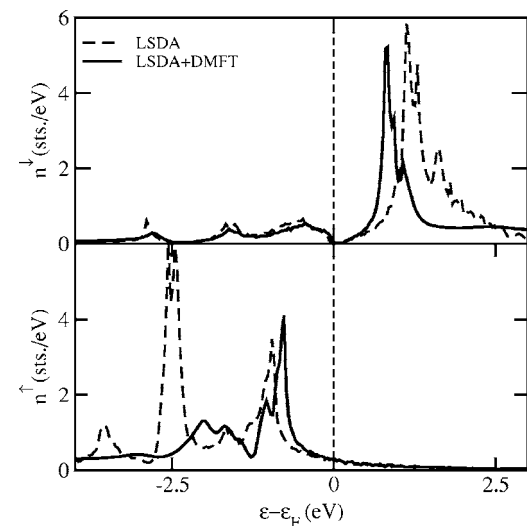


FIG. 3. Spin-resolved DOS of the Mn *d* shell. Broken line, LSDA calculations; solid line, LSDA+DMFT calculations.

Kerr effect to the modifications in the interband contribution of optical conductivity caused by the renormalization of the one-particle spectrum which is shown in Fig. 3. The false peak inserted by DMFT at 3 eV could be attributed first of all to the lack of vertex corrections in our calculation scheme. In order to describe the optical transitions correctly, the two-particle Green's function has to be used. That is because the expression (2) formulated in terms of the one-particle Green's function is an approximation which needs to be fully filled with the appropriate vertex corrections.³¹ However, the account of local correlations makes the implementation of vertex corrections in the computational scheme rather complicated and needs a separate investigation. An-

other aspect which might be interesting to investigate is the account of nonlocal correlations. In conclusion, it has been demonstrated that an improved description of correlation effects on the basis of the LSDA+DMFT scheme leads to a substantially improved agreement of the theoretical and experimental MO spectra.

This work was funded by the German BMBF (Bundesministerium für Bildung und Forschung) under Contract No. FKZ 05 KS1WMB/1. One of the authors (L.C.) acknowledges financial support by the Austrian Science Foundation (FWF Project P18505–N16) and CNCSIS.

*Present address: Faculty of Science, University of Oradea, RO-410087 Oradea, Romania.

- ¹P. G. van Engen, K. H. J. Buschow, R. Jongebreur, and M. Erman, *Appl. Phys. Lett.* **42**, 202 (1983).
- ²P. G. van Engen, Ph.D. thesis, Technical University Delft, 1983.
- ³R. Ohyama, T. Koyanagi, and K. Matsubara, *J. Appl. Phys.* **61**, 2347 (1987).
- ⁴P. P. J. van Engelen, D. B. de Mooij, J. H. Wijngaard, and K. H. J. Buschow, *J. Magn. Magn. Mater.* **130**, 247 (1994).
- ⁵J. van Ek and J. M. Maclaren, *Phys. Rev. B* **56**, R2924 (1997).
- ⁶M. C. Kautzky and B. M. Clemens, *Appl. Phys. Lett.* **66**, 1279 (1995).
- ⁷P. M. Oppeneer, V. N. Antonov, T. Kraft, H. Eschrig, A. N. Yaresko, and A. Y. Perlov, *Solid State Commun.* **94**, 255 (1995).
- ⁸V. N. Antonov, P. M. Oppeneer, A. N. Yaresko, A. Ya. Perlov, and T. Kraft, *Phys. Rev. B* **56**, 13012 (1997).
- ⁹X. Gao, J. A. Woollam, R. D. Kirby, D. J. Sellmyer, C. T. Tanaka, J. Nowak, and J. S. Moodera, *Phys. Rev. B* **59**, 9965 (1999).
- ¹⁰S. Picozzi, A. Continenza, and A. J. Freeman, *J. Phys. D* **39**, 851 (2006).
- ¹¹E. T. Kulatov, Y. A. Uspenskii, and S. V. Halilov, *Phys. Lett. A* **125**, 267 (1994).
- ¹²Y. A. Uspenskii, E. T. Kulatov, and S. V. Khalilov, *JETP* **80**, 952 (1995).
- ¹³A. Perlov, S. Chadov, and H. Ebert, *Phys. Rev. B* **68**, 245112 (2003).
- ¹⁴A. Perlov, S. Chadov, H. Ebert, L. Chioncel, A. I. Lichtenstein, and M. I. Katsnelson, *J. Magn. Magn. Mater.* **272**, 523 (2004).
- ¹⁵L. Chioncel, M. I. Katsnelson, R. A. de Groot, and A. I. Lichtenstein, *Phys. Rev. B* **68**, 144425 (2003).
- ¹⁶A. Georges, G. Kotliar, W. Krauth, and M. J. Rozenberg, *Rev. Mod. Phys.* **68**, 13 (1996); G. Kotliar and D. Vollhardt, *Phys. Today* **57** (3), 53 (2004).
- ¹⁷J. L. Erskine, E. A. Stern, *Phys. Rev. B* **12**, 5016 (1975).
- ¹⁸L. Szunyogh and P. Weinberger, *J. Phys.: Condens. Matter* **11**, 10451 (1999).
- ¹⁹R. Kubo, *J. Phys. Soc. Jpn.* **12**, 570 (1957); D. A. Greenwood, *Proc. Phys. Soc. London* **71**, 585 (1958).
- ²⁰T. Huhne, C. Zecha, H. Ebert, P. H. Dederichs, and R. Zeller, *Phys. Rev. B* **58**, 10236 (1998).
- ²¹P. W. Anderson, *Phys. Rev.* **124**, 41 (1961).
- ²²W. Metzner and D. Vollhardt, *Phys. Rev. Lett.* **62**, 324 (1989).
- ²³S. Biermann, F. Aryasetiawan, and A. Georges, *Phys. Rev. Lett.* **90**, 086402 (2003).
- ²⁴O. K. Andersen, *Phys. Rev. B* **12**, 3060 (1975).
- ²⁵N. E. Bickers and D. J. Scalapino, *Ann. Phys. (N.Y.)* **193**, 206 (1989).
- ²⁶A. I. Lichtenstein and M. I. Katsnelson, *Phys. Rev. B* **57**, 6884 (1998); M. I. Katsnelson and A. I. Lichtenstein, *J. Phys.: Condens. Matter* **11**, 1037 (1999); *Eur. Phys. J. B* **30**, 9 (2002).
- ²⁷J. Minár, L. Chioncel, A. Perlov, H. Ebert, and M. I. Katsnelson, and A. I. Lichtenstein, *Phys. Rev. B* **72**, 045125 (2005).
- ²⁸S. Biermann, A. Dallmeyer, C. Carbone, W. Eberhardt, C. Pam-puch, O. Rader, M. I. Katsnelson, and A. I. Lichtenstein, *JETP Lett.* **80**, 612 (2004); L. V. Pourovskii, M. I. Katsnelson, and A. I. Lichtenstein, *Phys. Rev. B* **73**, 060506(R) (2006).
- ²⁹L. V. Pourovskii, M. I. Katsnelson, and A. I. Lichtenstein, *Phys. Rev. B* **72**, 115106(R) (2005).
- ³⁰J. E. Hirsch, R. M. Fye, *Phys. Rev. Lett.* **56**, 2521 (1986); K. Held, I. A. Nekrasov, N. Blümer, A. Anisimov, and D. Vollhardt, *Int. J. Mod. Phys. B* **15**, 2611 (2001).
- ³¹G. Mahan, *Many-Particle Physics* (Plenum Press, New York, 1990), Chap. 8.